

Optical activity in planar chiral metamaterials

J. Petschulat,* A. Chipouline, A. Tünnermann,[†] and T. Pertsch
*Institute of Applied Physics, Friedrich-Schiller-Universität Jena,
Max Wien Platz 1, 07743, Jena, Germany*

C. Rockstuhl, C. Menzel, T. Paul, and F. Lederer
*Institute for Condensed Matter Theory and Solid State Optics,
Friedrich-Schiller-Universität Jena, Max Wien Platz 1, 07743, Jena, Germany*

(Dated: March 23, 2022)

Abstract

We present a detailed investigation of the optical properties of planar metamaterials in terms of a simple but accurate model. Therefore we rely on a mesoscopic description of the metaatom itself in terms of an auxiliary carrier distribution interacting with the illuminating radiation. Thus the effective parameters of the metamaterial can be determined with the knowledge of the far field intensities only. In a second step the metaatom geometry is modified in order to enable optical activity. We show that the anisotropic effective parameters can be predicted by considering these geometrical modifications in the auxiliary carrier setup. As an example we apply the formalism to explain the asymmetric transmission for left and right handed circular polarized light for this type of planar anisotropic metamaterials. Finally we show that the mesoscopic model reveals an important symmetry relation, namely the Onsager Casimir principle.

PACS numbers: 78.20.Ek, 41.20.Jb, 42.25.Ja

Keywords: Metamaterials, Optical activity, Chirality

INTRODUCTION

Metamaterials enrich the optical material response of naturally available media, since they access tailored macroscopic electromagnetic wave propagation by the microscopic control over the geometrical and dispersive properties of the metaatoms it is build of. The advantage of such artificial materials is that novel effects such as negative refraction [1, 2, 3], optical cloaking [4, 5, 6, 7, 8, 9], as well as a series of optical analogues to phenomena known from different disciplines in physics become amenable [10, 11, 12, 13].

Beginning from the pioneering metaatoms working in the optical domain the diagonal anisotropic response [1, 2, 3, 14, 15, 16] with respect to the effective material parameter tensor (linear dichrosim) has been recently extended towards the anisotropic regime sustaining off-diagonal elements (elliptical dichrosim). This extension dramatically changes the wave propagation in such a media and evokes several physical phenomena, e.g. optical activity [17, 18, 19, 20, 21], bidirectional and anti-symmetric transmittance [22, 23, 24] or chirality induced negative refraction [25, 26, 27]. In order to predict and explore such novel features by this new type of effective media numerical rigorous computational techniques are applied that allows to determine the near and far field properties.

The intrinsic drawback of such an analysis is that the optical response, e.g. the transmittance or the reflectance, directly follows from defining the geometrical parameters and the bulk material properties of the microscopic metaatoms while the effective material tensors in general remain unknown. The knowledge about this would be vital for gaining a deeper understanding about the wave interaction with this artificial type of media in the same manner as the understanding of ordinary metamaterials benefits from their associated effective material parameters. In order to reveal the nature of these observables a few approaches have been proposed incorporating, e.g. Lorentz electronic theory [23] or the analogy to optical chirality observed by molecules by an effective medium treatment [17]. In contrast to these *bottom up* approaches the rigorous determination of such parameters in terms of an effective material parameter retrieval is quite complex [28] and requires sophisticated experimental techniques, i.e. phase resolved measurements.

Hence our purpose is to introduce a simple but accurate model correlating the metaatoms intrinsic dynamics with their associated effective material properties. This allows us to link the far field properties to the specific plasmonic eigenmodes and to investigate microscopic

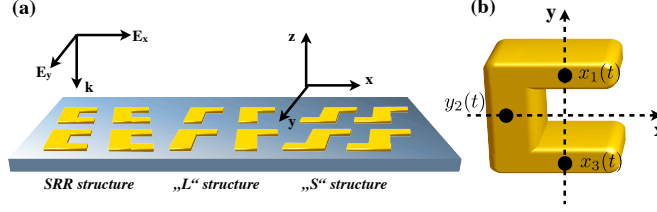


FIG. 1: **(a)** The original SRR structure (left), the first modification, namely the L (center) and the second modification, the S structure (right). **(b)** The SRR together with its auxiliary carrier setup, sketched by the black dots.

manipulations on the metaatom and their effect on the anisotropic material properties. We start our investigation with an optical non-active anisotropic metamaterial geometry, namely the split-ring resonator (SRR). In the following different structural modifications enabling optical activity are covered and related to the initial SRR material properties. As an application of these parameters we discuss the anti-symmetric transmittance for the optical active modifications and compare an effective medium slab sustaining the before mentioned effective parameters with rigorous simulations of the structure. Since for all considerations an excellent agreement is observed and the method bases only on intensity values for the far field observables we suggest this method as a potential parameter retrieval procedure. In the end we can directly verify that the predictions following from such a model are valid in terms of the Casimir-Onsager relations [29, 30]; the requirement for time reversal and reciprocity in linear media [31].

THE PLANAR SRR STRUCTURE

At first we substitute the planar SRR geometry, shown in FIG.(1b), by a chain of coupled carriers

$$\begin{aligned}
 \frac{\partial^2}{\partial t^2}x_1 + \gamma_1 \frac{\partial}{\partial t}x_1 + \omega_1^2x_1 + \sigma_{21}y_2 &= -\frac{q_1}{m}E_x, \\
 \frac{\partial^2}{\partial t^2}y_2 + \gamma_2 \frac{\partial}{\partial t}y_2 + \omega_2^2y_2 + \sigma_{21}x_1 + \sigma_{23}x_3 &= -\frac{q_2}{m}E_y, \\
 \frac{\partial^2}{\partial t^2}x_3 + \gamma_3 \frac{\partial}{\partial t}x_3 + \omega_3^2x_3 + \sigma_{23}y_2 &= -\frac{q_3}{m}E_x
 \end{aligned} \tag{1}$$

where we have assumed nearest neighbor coupling between adjacent, i.e. electrically connected, charges. In general the illumination of the structure is provided by an electric field

propagating in z direction, whereas the magnetic field coupling can be neglected [32, 33]. In Eqs.(1) γ_j is the damping, ω_{0j} the eigenfrequency and σ_{ij} the coupling constant for the three respective carriers $(i, j) \in (1, 2, 3)$, similarly to those introduced in [33]. Together with the multipole definitions [34] incorporating the electric dipole moment

$$\begin{aligned}\mathbf{P}(\mathbf{r}, t) &= \eta \sum_{l=1}^N q_l \mathbf{r}_l, \\ \mathbf{P}(\mathbf{r}, \omega) &= \epsilon_0 \chi_{ij}(\omega) \mathbf{E}(\mathbf{r}, \omega)\end{aligned}\quad (2)$$

and the wave equation

$$\begin{aligned}\Delta \mathbf{E}(\mathbf{r}, \omega) &= -\mu_0 \epsilon_0 \omega^2 \mathbf{E}(\mathbf{r}, \omega) - \omega^2 \mu_0 \mathbf{P}(\mathbf{r}, \omega) \\ &+ \omega^2 \mu_0 \nabla \cdot \mathbf{Q}(\mathbf{r}, \omega) - i\omega \mu_0 \nabla \times \mathbf{M}(\mathbf{r}, \omega)\end{aligned}\quad (3)$$

we are able to calculate the effective parameters. Whereas η in Eqs.(2) accounts for the number density of electric dipoles. We put emphasis on the fact that there are appearing higher order multipole moments (Q, M), but they are not contributing to the wave equation Eq.(3) for this particular propagation direction. Thus there is no effective magnetic response by means of the effective magnetic permeability as it has been intensively discussed elsewhere [35]. This implies (regarding the material equations) that the complex and homogeneous effective susceptibility tensor Eq.(2) is connected to the effective permittivity tensor by

$$\epsilon_{ij}(\omega) = \mathbf{1} + \chi_{ij}(\omega). \quad (4)$$

Moreover the vanishing of second order multipoles allows to obtain the dispersion relation as well as the effective refractive index as usual for plane wave propagation from the wave equation Eq.(3) in the electric dipole limit $k(\omega)_{ij} = \omega c^{-1} \sqrt{\epsilon_{ij}(\omega)} = \omega c^{-1} n_{ij}(\omega)$ for normal incidence. At first we consider the possible carrier eigenmodes for the two polarization directions (x, y) . In order to describe a SRR with two identical SRR arms we set $\omega_{01} = \omega_{03} \equiv \omega_{0x}$, $\gamma_1 = \gamma_3 \equiv \gamma_x$, $\sigma_{21} = \sigma_{23}$ and $q_1 = q_3 \equiv -q_x$ and for the remaining parameters $\omega_{02} \equiv \omega_{0y}$, $\gamma_2 \equiv \gamma_y$ and $q_2 \equiv -q_y$. The discrimination of the SRR arm (the two wires in x direction) and SRR base (wire in y direction) parameters tributes the geometrical difference of the SRR dimensions, which would not be necessary for the trivial case of an equal arm width along the entire structure. For a polarization parallel to the x axis we can solve Eqs.(1)

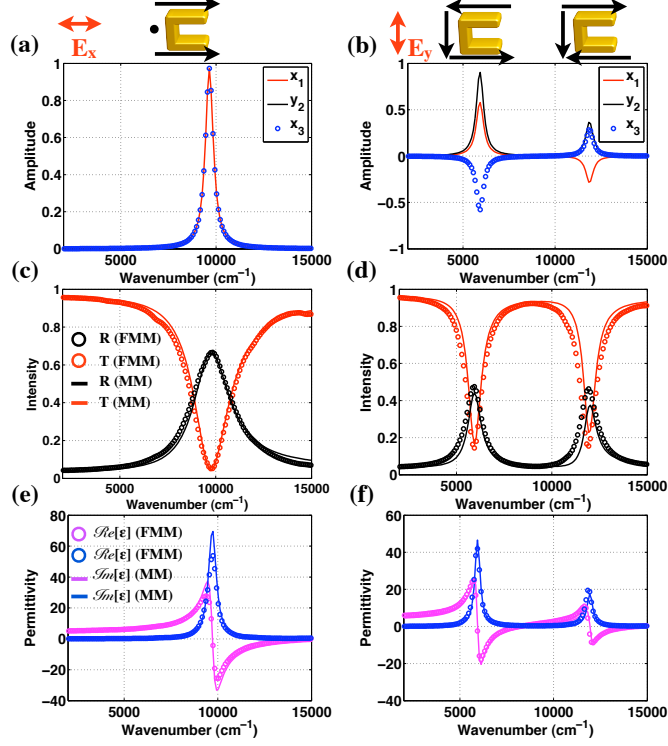


FIG. 2: (a) The solution for the carrier oscillation amplitudes (normalized) for a polarization along the SRR arms (x) and perpendicular (y) (b). (c),(d) The respective calculated and analytical obtained SRR far field spectra for these particular polarizations and the exactly retrieved parameters compared to its analytical counterparts (e),(f).

and obtain the following oscillation amplitudes in Fourier domain [$a(t) = a(\omega)\exp(-i\omega t)$]

$$\begin{aligned}
 x_1(\omega) &= -\frac{q_y}{m} \frac{1}{A_x} E_x(z, \omega), \\
 y_2(\omega) &= 0, \\
 x_3(\omega) &= x_1(\omega), \\
 A_x &\equiv \omega_{0x}^2 - \omega^2 - i\omega\gamma_x.
 \end{aligned} \tag{5}$$

For a polarization in y direction we get the carriers oscillation amplitudes according to

$$\begin{aligned}
 x_1(\omega) &= -\frac{q_y}{m} \frac{\sigma}{A_x A_y(\omega) - 2\sigma^2} E_y(z, \omega), \\
 y_2(\omega) &= -\frac{q_y}{m} \frac{A_x(\omega)}{A_x A_y(\omega) - 2\sigma^2} E_y(z, \omega), \\
 x_3(\omega) &= -x_1(\omega), \\
 A_y &\equiv \omega_{0y}^2 - \omega^2 - i\omega\gamma_y.
 \end{aligned} \tag{6}$$

Considering the eigenmodes for x polarization we observe that two parallel dipoles ($x_1 = x_3$) are induced, while there is no elongation in y direction ($y_2 = 0$) Eqs.(5), FIG.(2a). In contrast to this a y polarized illumination induces besides the parallel carrier motion in y direction an oscillation in x direction, but due to the anti-symmetric oscillation ($x_3 = -x_1$) [FIG.(2b)] Eqs.(6) the SRR arms in terms of their associated electric dipole response do not radiate. Thus there is no induced cross polarization such as x polarized radiation induces an electric dipole in y direction and vice versa. Later we will prove directly that emerging xy , yx contributions will result in optical activity, as expected.

By substituting Eqs.(5, 6) in Eqs.(2) we get the expected diagonal susceptibility tensor for the SRR carrier configuration

$$\chi(\omega) = \begin{pmatrix} \chi_{xx}(\omega) & 0 & 0 \\ 0 & \chi_{yy}(\omega) & 0 \\ 0 & 0 & 0 \end{pmatrix},$$

$$\chi_{xx}(\omega) = \frac{q_x^2 \eta}{m \epsilon_0} \frac{2}{A_x(\omega)},$$

$$\chi_{yy}(\omega) = \frac{q_y^2 \eta}{m \epsilon_0} \frac{A_x(\omega)}{A_x(\omega) A_y(\omega) - 2\sigma^2}. \quad (7)$$

with the dipole moment according to Eqs.(2) $\mathbf{P} = -\eta (q_x(x_1 + x_3), q_y y_2, 0)^T$. In order to prove the validity of these considerations, we performed numerical Fourier Model Method (FMM) calculations [36] of a periodical array of gold SRR's [45] similar to those reported in [2]. Thereon the numerical far field observables (T, R) have been fitted by substituting the effective permittivity tensor Eq.(4) for the two polarization directions (x, y) within a conventional transfer matrix formalism. In FIG.(2) the transition of the eigenmodes denoted as resonances within the oscillation amplitudes towards their effect on the reflection and transmission spectra, and finally their influence on the effective parameters becomes evident. We note that the unknown oscillator parameters can be found by comparing the far field intensity only, which can be understood similar to the conventional parameter retrieval procedure, but without the necessity of knowing the complex valued fields. This will be advantageous for optical active structures where the determination of these parameters is in general costly. Finally we observe that the exactly calculated spectra as well as the exactly retrieved parameters nicely coincide with their corresponding analytical values.

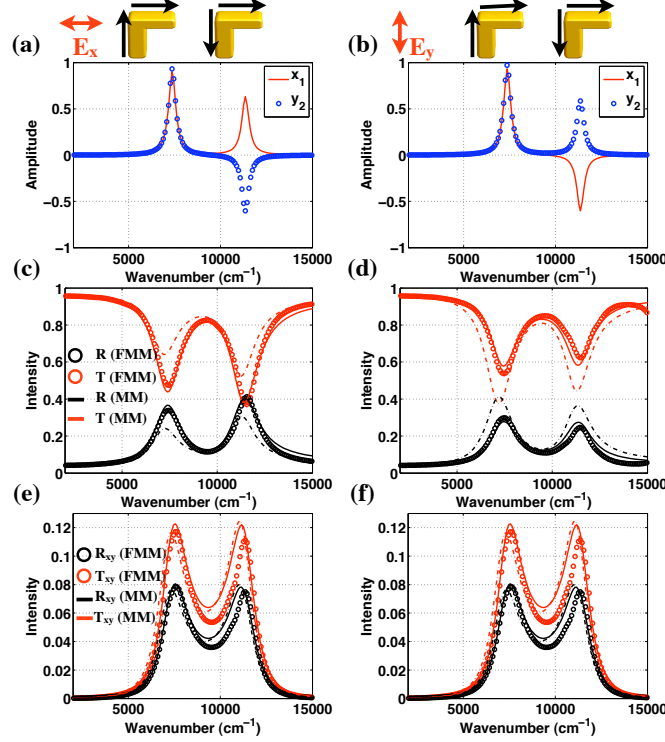


FIG. 3: (a) The L structure eigenmodes for x and (b) for y polarization. In contrast to the SRR both eigenmodes are excited for each polarization direction, simultaneously. (c),(d) The calculated (spheres); analytical predicted (dashed-dotted) applying the SRR parameters; and the fitted far field response for the two polarizations. The respective numerical cross-polarization contributions compared with the model predicted values (e),(f).

PLANAR MODIFICATIONS: THE "L" STRUCTURE

In order to extend the previous considerations towards optical active effective media we perform the first modification on the SRR structure yielding the L structure [37, 38]. Thereby we have dropped one SRR arm in order to prevent the cancellation of the dipole moments in both SRR arms as it has been observed before, e.g. for y polarization Eqs.(6). Considering the set of coupled oscillator equations Eqs.(1) this is coherent with disregarding one horizontal oscillating carrier, e.g. carrier 3. We now obtain the carrier amplitudes for x

$$\begin{aligned}
 x_1^x &= -\frac{q_x}{m} \frac{A_y(\omega)}{A_x(\omega)A_y(\omega) - \sigma^2} E_x(z, \omega), \\
 y_2^x &= -\frac{q_x}{m} \frac{\sigma}{A_x(\omega)A_y(\omega) - \sigma^2} E_x(z, \omega)
 \end{aligned} \tag{8}$$

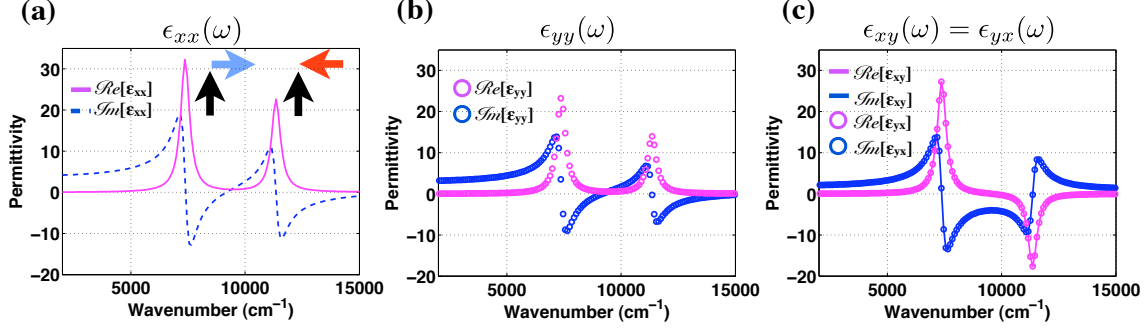


FIG. 4: The diagonal effective permittivity tensor elements $\epsilon(\omega)_{xx}$ (a) and $\epsilon(\omega)_{yy}$ (b). The sketched arrows indicate the current flow, represented by the carrier oscillation direction for the particular eigenmode resonance. (c) The off-diagonal elements $\epsilon(\omega)_{ij}$ comprising a Lorentz resonance around $\bar{\nu} = 7,000 \text{ cm}^{-1}$ and an anti-Lorentz resonance at $\bar{\nu} = 11,000 \text{ cm}^{-1}$.

and for y polarization

$$\begin{aligned} x_1^y &= -\frac{q_y}{m} \frac{\sigma}{A_x(\omega)A_y(\omega) - \sigma^2} E_y(z, \omega), \\ y_2^y &= -\frac{q_y}{m} \frac{A_x(\omega)}{A_x(\omega)A_y(\omega) - \sigma^2} E_y(z, \omega). \end{aligned} \quad (9)$$

Together with the resulting dipole moment Eqs.(2)

$$\mathbf{P}^j(z, \omega) = -\eta \begin{pmatrix} q_x x_1^j \\ q_y y_2^j \\ 0 \end{pmatrix}, \quad j \in [x, y] \quad (10)$$

the susceptibility can be obtained to

$$\begin{aligned} \chi(\omega) &= \begin{pmatrix} \chi_{xx}(\omega) & \chi_{xy}(\omega) & 0 \\ \chi_{yx}(\omega) & \chi_{yy}(\omega) & 0 \\ 0 & 0 & 0 \end{pmatrix}, \\ \chi_{xx}(\omega) &= \frac{q_x^2 \eta}{m \epsilon_0} \frac{A_y(\omega)}{A_x(\omega)A_y(\omega) - \sigma^2}, \\ \chi_{yy}(\omega) &= \frac{q_y^2 \eta}{m \epsilon_0} \frac{A_x(\omega)}{A_x(\omega)A_y(\omega) - \sigma^2}, \\ \chi_{xy}(\omega) &= \frac{q_x q_y \eta}{m \epsilon_0} \frac{\sigma}{A_x(\omega)A_y(\omega) - \sigma^2}, \\ \chi_{yx}(\omega) &= \frac{q_x q_y \eta}{m \epsilon_0} \frac{\sigma}{A_x(\omega)A_y(\omega) - \sigma^2}. \end{aligned} \quad (11)$$

The most significant change compared to the SRR is the appearance of cross polarization contributions, i.e. $\chi_{ij}(\omega)$. Moreover we observe that the susceptibility tensor Eqs.(11) and with it the effective permittivity Eq.(4) is symmetric $\chi_{ij}(\omega) = \chi_{ji}(\omega)$. This symmetry relation is important since it is the requirement for time reversal, known as the Onsager-Casimir principle [29, 30, 31]. Additionally we mention that the tensor has the same mathematical form as expected for planar optical active media [17, 23]. Regarding the oscillator amplitudes Eqs.(8, 9) we mention that this symmetry cannot be observed for the charge eigenmodes, since $y_2^x \neq x_1^y$ as long as $q_x \neq q_y$ (which accounts for the oscillator strength). But due to the dipole moment both quantities are multiplied with the opposite charge which equalizes both contributions ($q_y y_2^x = q_x x_1^y$). Another difference with respect to the SRR is that the splitting σ between both resonances is reduced (by a factor of $\sqrt{2}$), which follows from neglecting one of the SRR arms.

In order to check whether such a description is valid and to reveal the relationship between the SRR and the L structure eigenmodes, we performed again numerical FMM simulations for the L structure and compared the results to the analytical model FIG.(3). It is important to note that for the analytical calculations of the spectra the ordinary transfer matrix formalism applied for the SRR before does not hold any longer since we require now a formalism that accounts for the full tensorial character of $\epsilon_{ij}(\omega)$ [39]. This fact is a major reason for the complexity of rigorously retrieving effective parameters for general anisotropic media. Nevertheless the analytical spectral calculations shown in FIG.(3c-f) have been performed twice. At first we utilized all the found parameters from the SRR structure without further fitting, which predicts the dashed-dotted lines FIG.(3c-d). Although there are deviations between these results and the exact numerical calculations the qualitative agreement, e.g. for the resonance positions becomes obvious. In a second step we adapted these parameters in order to fit the exact calculations [solid lines in FIG.(3c-d)] providing an almost perfect coincidence with the numerical values [46]. In a final step we compared the cross-polarization contributions (T_{ij} , R_{ij}) with the predicted behavior incorporating the parameters found for the regular diagonal parameters (T_{ii} , R_{ii}) [FIG.(3e,f)]. The agreement between these cross-polarization terms prove that the description presented here significantly differs from fitting the electric response by several Lorentz-shaped functions adapted to coincide with the far fields response. With our approach the real plasmon dynamics are mapped onto a supplementary carrier setup that is able to cover also complex eigenmodes that are responsible for

the appearance of cross-polarization contributions. In the last step we can provide the effective permittivity tensor, that is inherently accessible and already applied in order to fit the spectra, FIG.(4). It can be deduced that for the two polarization directions the two eigenmodes denoted as Lorentz-shaped resonances within the effective permittivities are present but differ in strength, due to the different geometrical parameters of the L arms FIG.(4a,b). The off-diagonal elements $\epsilon(\omega)_{ij}$ are equal as discussed before, [FIG.(4c)]. Considering especially the second resonance at around $\bar{\nu} = 11,000 \text{ cm}^{-1}$ for the off-diagonal tensor elements, we observe a negative Lorentz resonance, that might suggest any gain within the system due to the negative imaginary part. The nature of this resonance is strictly linear and can be explained with the introduced formalism as well. Since the permittivity is proportional to the susceptibility Eq.(4) and with this also to the carrier amplitudes Eqs.(11), a negative sign can be understood by a phase difference of π between the the two oscillating carriers, thus both are oscillating in opposite directions, while for the positive Lorentz resonance at around $\bar{\nu} = 7,000 \text{ cm}^{-1}$, both carriers are oscillating in phase [sketched by the arrows in FIG.(4a)].

PLANAR MODIFICATIONS: THE "S" STRUCTURE

The following modification is not aiming at producing additional physical effects compared to the L structure, but completes our idealized description with an optical active structure that can be obtained preserving the number of supplementary carriers as introduced for the SRR. Similar to the L structure we must prevent that parallel carrier oscillations annihilate in order to observe cross-polarization contributions, required of optical active metaatoms. Therefore we mirror one of the SRR arm carriers (e.g. x_3) with respect to the SRR basis, yielding the S structure [40, 41] FIG.(1a). This *opening* of the SRR structure is expected to enable the observation of two modes for x polarization, since the center carrier (y_2) can now oscillate in line or contrarily with the carriers in the top and bottom S structure wires that are excited by the x polarized electric field. For y polarization the situation is comparable, but now the two horizontal carriers (x_1, x_3) are allowed to oscillated in line or contrarily to the electric field excited carrier motion (y_2). Mathematically this change can be considered by setting $\sigma_{23} = -\sigma_{21} \equiv -\sigma$, while all other parameters appear similar to the ones applied for the SRR. Physically this can be understood by regarding Eqs.(1), where

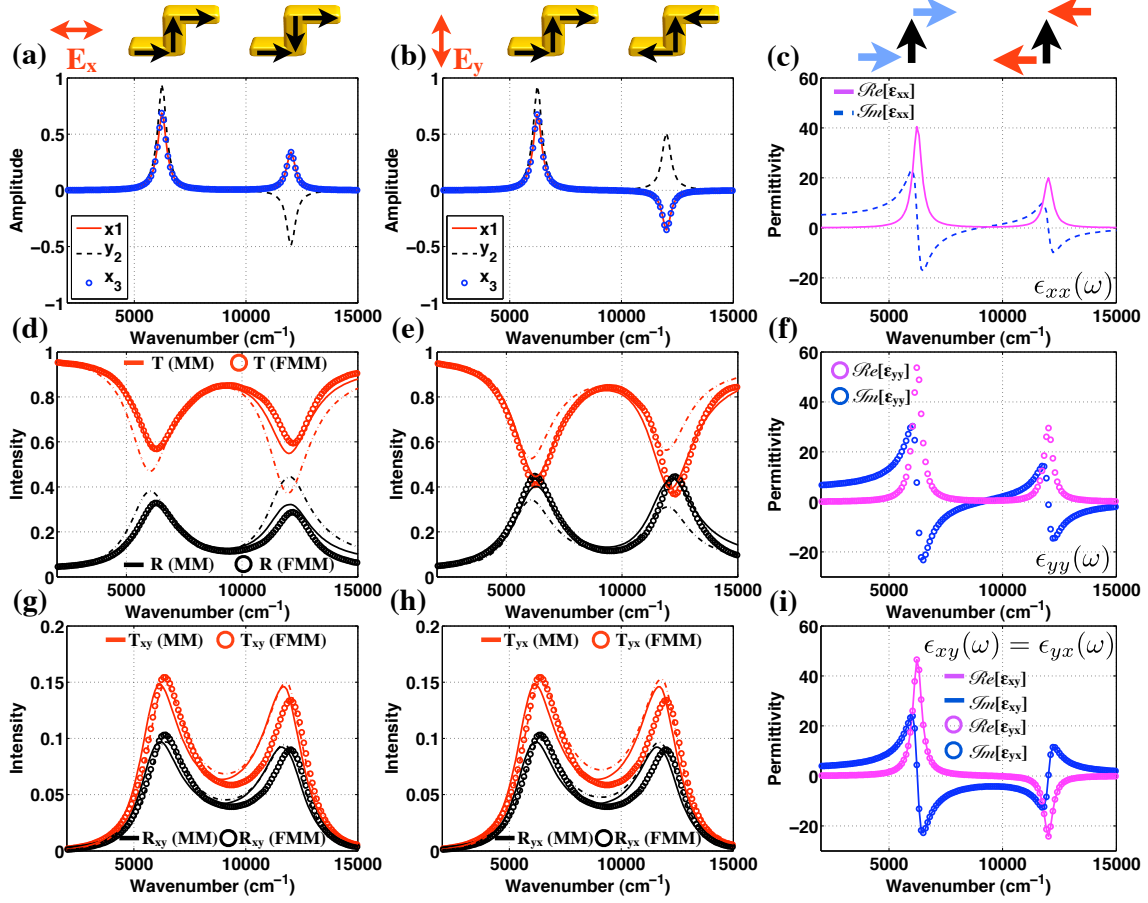


FIG. 5: The carrier eigenmodes, i.e. an in line elongation over the entire structure and a contrary elongation with respect to the center part of the S structure are observed for the two polarization directions x (a) and y (b). (d), (e) The far field spectra obtained by numerical simulations (circles); by the predictions based on the SRR structure parameters (dashed-dotted lines); and by adapting the parameters to fit the numerical values (solid lines). The comparison between the cross-polarization contribution (T_{ij} , R_{ij}) between the numerical simulations (circles) and the model (solid lines) for the found parameters deduced for fitting the diagonal response (T_{ii} , R_{ii}). The effective permittivity tensor diagonal (c), (f) and the off-diagonal components (i).

for a positive elongation of charge 1 ($y_2 > 0$) the lower SRR arm charge 3 is accelerated in negative direction ($x_3 < 0$). For the S structure the behavior is inverse, thus a positive elongation of y_2 induces an acceleration in positive direction for charge x_3 . Hence the force described by the coupling constant must be inverted, which is equivalent to changing the sign of σ_{23} . Beginning from here all calculations can be repeated in analogy to the calculations for the SRR and the L structure before. Thus we obtain the oscillator amplitudes for

x polarization

$$\begin{aligned}
x_1^x &= -\frac{q_x}{m} \frac{A_y(\omega)}{A_x(\omega)A_y(\omega) - 2\sigma^2} E_x(z, \omega), \\
y_2^x &= -\frac{q_x}{m} \frac{2\sigma}{A_x(\omega)A_y(\omega) - 2\sigma^2} E_x(z, \omega), \\
x_3^x &= x_1^x
\end{aligned} \tag{12}$$

and for y polarization

$$\begin{aligned}
x_1^y &= -\frac{q_y}{m} \frac{\sigma}{A_x(\omega)A_y(\omega) - 2\sigma^2} E_y(z, \omega), \\
y_2^y &= -\frac{q_y}{m} \frac{A_x(\omega)}{A_x(\omega)A_y(\omega) - 2\sigma^2} E_y(z, \omega), \\
x_3^y &= x_1^y
\end{aligned} \tag{13}$$

as well as the effective susceptibility tensor

$$\begin{aligned}
\chi(\omega) &= \begin{pmatrix} \chi_{xx}(\omega) & \chi_{xy}(\omega) & 0 \\ \chi_{yx}(\omega) & \chi_{yy}(\omega) & 0 \\ 0 & 0 & 0 \end{pmatrix}, \\
\chi_{xx}(\omega) &= \frac{q_x^2 \eta}{m \epsilon_0} \frac{2A_y(\omega)}{A_x(\omega)A_y(\omega) - 2\sigma^2}, \\
\chi_{yy}(\omega) &= \frac{q_y^2 \eta}{m \epsilon_0} \frac{A_x(\omega)}{A_x(\omega)A_y(\omega) - 2\sigma^2}, \\
\chi_{xy}(\omega) &= \frac{q_x q_y \eta}{m \epsilon_0} \frac{2\sigma}{A_x(\omega)A_y(\omega) - 2\sigma^2}, \\
\chi_{yx}(\omega) &= \frac{q_x q_y \eta}{m \epsilon_0} \frac{2\sigma}{A_x(\omega)A_y(\omega) - 2\sigma^2}.
\end{aligned} \tag{14}$$

In Eqs.(14) we have applied the electric dipole moment according to Eqs.(2) which is found to be exactly the same as for the SRR structure, while the carrier amplitudes are completely different. Regarding the splitting, we expect the same resonance displacement as for the SRR in y polarization, since 2σ appears in the denominator of the SRR oscillation amplitudes [Eqs.(7) for y polarization] as well as in all oscillator amplitudes in Eqs.(12) and Eqs.(13).

At this point we emphasize that the dipole moment is invariant with respect to any translation of the coordinate system as long as accompanied to the negative carriers, that are allowed to oscillate, fixed positive carriers are present. These positive carriers are required

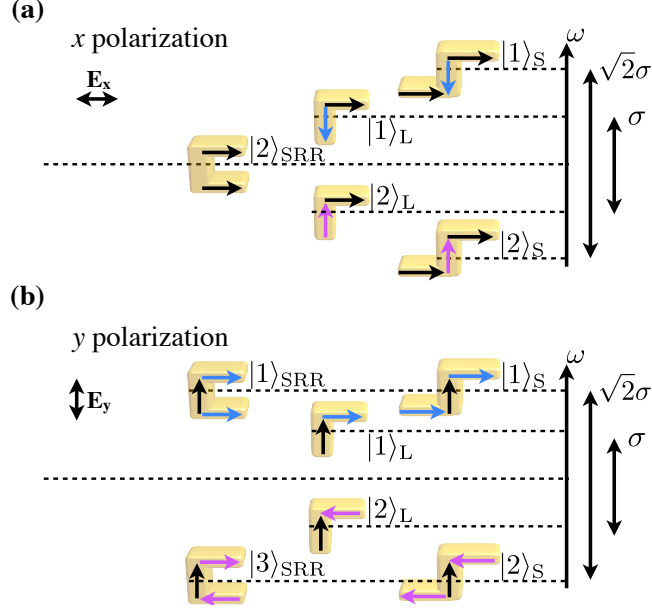


FIG. 6: The appearing eigenmodes for the three structures are categorized with respect to the excitation polarization [x (a) and y (b)]. It can be observed that the SRR exhibits three eigenmodes while the L and S structure posses two eigenmodes excitable for both polarization directions simultaneously. The symmetric splitting between all occurring modes can be captured by the coupling constant σ .

anyway since a neutral total charge is assumed for the entire structure. Otherwise the respective geometry would exhibit a constant dipole moment [Eqs.(2)], even without the presence of an electric field, which differs from the physical situation in regular metamaterials that we want to describe here.

Performing the respective numerical and analytical calculations as for the L structure before, we can predict the spectral response as well as the effective material properties based on the plasmonic eigenmodes FIG.(5). Considering these eigemodes FIG.(5a,b), we observe two situations. At first an eigenmode that represents a convective current along the entire S structure. The second eigenmode is determined by a parallel oscillation in the S structure arms accompanied with an opposite oscillation in the center part of the metaatom. Both eigenmodes are excited for x and y polarization respectively producing the spectral resonances denoted as transmission dips or reflection peaks FIG.(5d,e) with the expected frequency displacement equivalent to the SRR structure. We note that this in line eigenmode appears similar to the L structures in line eigenmode at shorter wavenumbers (larger

wavelengths) while the contrarily oscillating eigenmode is observed at larger wavenumbers (smaller wavelengths), FIG.(6). This is similar to the plasmon hybridization model developed for plasmonic nanostructures [42]. Qualitative this can be understood such as an in line carrier eigenmode takes advantage of an effective longer structure (the addition of all structure elements) producing a red shift while an contrary eigenmode exploits the single structure elements, thus the optical response is discriminated by effectively shorter structures yielding a blue shift of the resonance positions.

Again the application of the SRR oscillator parameters (dash-dotted lines) reveals the relationship between both structures, since the numerically (circles) calculated spectra agree with respect to the overall shape and the resonance positions FIG.(5d,e). Whereas a fitting again improves the coincidence towards almost excellent agreement, which can also be observed for the cross polarization observables FIG.(5g,h). Considering the tensor components of the effective permittivity, we observe a difference between the diagonal entries due to the geometrical differences in the S structure center and the S structure arms, while the anti-resonance for the contrary carrier eigenmode is observed in the off-diagonal elements with the same origin as discussed for the L structure.

ANTI-SYMMETRIC TRANSMITTANCE

In order to probe the optical activity induced by the before mentioned geometrical modifications on the SRR structure we calculate the transmission properties of the discussed structures for circular polarized light. Thus we expect for the L and S structure a different behavior for left handed circular polarized light (LCPL) as for right handed circular polarized light (RCPL) since the effective permittivity tensor is similar occupied as for biaxial elliptically dichroic crystals [23]. To obtain right handed and left handed circular polarized light we have to ensure a phase shift between the linear polarized light transmittances such as [27]

$$\begin{pmatrix} T_{rr} & T_{rl} \\ T_{lr} & T_{ll} \end{pmatrix} = \frac{1}{2} \begin{pmatrix} T_{xx} + T_{yy} + i(T_{xy} - T_{yx}) & T_{xx} - T_{yy} - i(T_{xy} + T_{yx}) \\ T_{xx} - T_{yy} + i(T_{xy} + T_{yx}) & T_{xx} + T_{yy} - i(T_{xy} - T_{yx}) \end{pmatrix}. \quad (15)$$

In Eq.(15) the index r denotes RCPL while l represents LCPL such as that, e.g. T_{rl} is the transmission coefficient from left to right handed circular polarized light. Considering

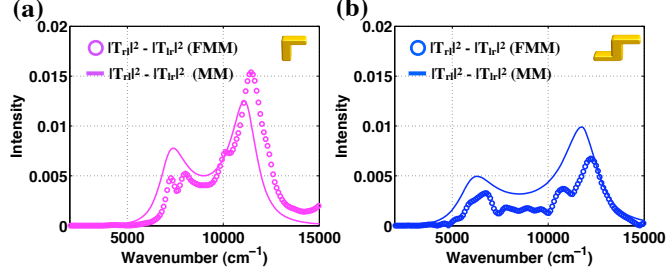


FIG. 7: The absolute transmission coefficient difference between $|T_{lr}|^2$ and $|T_{rl}|^2$ for the L (a) and the S (b) structure obtained by the permittivity tensor based calculations in comparison to the exact numerical results.

Eq.(15) it is obvious that for a diagonal effective permittivity tensor (linear dichroism) there is no difference between T_{rr} and T_{ll} since the cross polarization components vanish and with it $T_{xy} = T_{yx} = 0$. For non-vanishing off-diagonal entries of the permittivity tensor (elliptical dichroism) for the planar structures considered here these observables are symmetric yielding $T_{xy} = T_{yx}$. Thus there is still no difference between T_{rr} and T_{ll} but in contrast to this now $T_{rl} \neq T_{lr}$ as long as $T_{xx} \neq T_{yy}$ which can be tailored by the geometrical differences (or different material) in the structure composition, e.g. a symmetric L structure with two equal arms would provide this. Since for all structures covered here $T_{xx} \neq T_{yy}$, or in the language of the permittivity $\epsilon_{xx} \neq \epsilon_{yy}$ we expect a difference between the two circular polarized quantities expressed by T_{rl} and T_{lr} . Thus we have applied the known permittivity tensors as well as the numerically obtained transmittances in order to calculate all parameters required by Eq.(15) for the two optical active structures. The comparison between both in FIG.(7) reveals that the general physics, namely the localization of the effect around both plasmonic eigenmode resonances can be observed which proves the expected behavior from the above considerations. We add that the differences between the predicted values based on our model differs to the numerical values in an absolute accuracy of $< 0.5\%$.

SUMMARY

In summary we have presented a series of modifications on the SRR geometry that enables optical activity which all can be cast within a simple analytical framework. Therefore the exact metaatoms geometry was replaced by a suitable supplementary carrier setup, that in-

teracts with the illuminating radiation. At first we have shown for the SRR that by aligning the carriers the set of observable eigenmodes is determined and their effect on the far field spectra as well as on the effective parameters can be revealed. We found that although the plasmonic eigenmodes are differing in their nature with respect to their underlying carrier oscillations, they all can be mapped into the electric dipole response of the corresponding effective medium. Moreover the effective medium is non-magnetic in terms of any response within the effective permeability. This would require non-zero response of higher order multipole contributions, e.g. the electric quadrupole or equivalently the magnetic dipole moment representing the next order in the multipole expansion as it has been shown for the cut-wire structure [33] or the upright SRR configuration [43]. These modes are present but for the particular propagation direction presented here they are not contributing.

The effective material properties of the present SRR structure can be completely determined by comparing the far field intensities to an effective medium slab described by the effective response provided by the supplementary carrier distribution. With the knowledge about these parameters two modifications on the initial SRR enable optical activity by the appearance of cross polarization terms. Due to the fact that we consider planar metamaterials incorporating a non-magnetic response the Onsager-Casimir principle requires the symmetry of the permittivity tensors for this class of planar geometries [31]. Hence we could observe that our model accounts for these restrictions inherently for all modifications. We note that for general bianisotropic media sustaining additionally an anisotropic magnetic response the requirements following from this principle are much more complex.

In a second step we simultaneously considered all planar modifications at the SRR within the supplementary carrier setup for the L and S structure. Since we consider for all structures differing substrate ($n = 1.5$) and ambient ($n = 1$) materials the two modified structures represent planar chiral (L) and non-chiral (S) metaatoms both supporting optical activity as expected. The induced changes point out that the optical activity can be understood in terms of the coupling induced launching of perpendicular dipole moments with respect to the incident polarization direction. The correlated radiation of these dipoles is polarized perpendicular to the incident polarization yielding the associated cross-polarization contributions accompanied with off-diagonal entries in the permittivity tensor. This allows us to estimate the optical response of both structures with the knowledge of the microscopic carrier parameters fixed from the SRR structure. A direct fit to the far field spectral response

provides an excellent agreement. This fitting procedure allows us to obtain the complete permittivity tensor based on the adaption of the far field intensities only. This procedure has several advantages, e.g. the system is probed by two perpendicular linear polarizations (and not by their elliptical polarized eigenstates) and only the far field intensities are required. For the comparison with numerical calculations the latter is not important since complex valued fields are usually obtained with the same effort as the intensities, but for the comparison with experimental values this method simplifies the access to such effective parameters dramatically.

Finally we applied the effective material tensor in order to calculate the difference in transmission for left and right handed polarized light. The knowledge about the explicit tensorial character enables us to probe the effect of the respective entries explicitly. Thus we could show that the difference for circular polarized waves can be assigned to the off-diagonal effective permittivity tensor entries as expected and that we observe a sufficient agreement between numerical calculations.

Finally we wish to add that the present approach represents a further step towards a simple theoretical model system to explain the optical response of complex shaped metamaterials in a mesoscopic limit. Thus all applied techniques, e.g. the multipole expansion as well as the coupled harmonic oscillator setup, are known and simple tools that allow to gain both a physical understanding and appropriate results based on an intuitive picture of the appearing effects. Hence this paper extends already present and related works covering the linear (electric and magnetic) response [33] as well as the possible consideration of nonlinear effects [43] towards optically active structures.

ACKNOWLEDGEMENTS

Financial support by the Federal Ministry of Education and Research as well as from the State of Thuringia within the Pro-Excellence program is acknowledged.

* Electronic address: joerg.petschulat@uni-jena.de

† also with: Fraunhofer Institute of Applied Optics and Precision Engineering Jena, Germany.

[1] Yuan, W. Cai, S. Xiao, V. Drachev, and V. Shalaev, *Opt. Lett.* **32**, 1671 (2007).

- [2] G. Dolling, M. Wegener, and C. Soukoulis, *Opt. Lett.* **32**, 53 (2007).
- [3] J. Valentine, S. Zhang, T. Zentgraf, G. B. E Ulin-Avila, Dentcho A. Genov, and X. Zhang, *Nature* **455**, 376 (2008).
- [4] J. Valentine, J. Li, T. Zentgraf, G. Bartal, and X. Zhang, *Nature Mat.* **8**, 568 (2009).
- [5] A. Alù and N. Engheta, *Phys. Rev. Lett.* **102**, 1 (2009).
- [6] Y. Lai, J. Ng, H. Chen, D. Han, J. Xiao, Z.-Q. Zhang, and C. T. Chan, *Phys. Rev. Lett.* **102**, 1 (2009).
- [7] M. Farhat, S. Guenneau, and S. Enoch, *Phys. Rev. Lett.* **103**, 1 (2009).
- [8] Justice, S. Cummer, J. Pendry, and A. Starr, *Science* **314**, 977 (2006).
- [9] U. Leonhardt, *Science* **312**, 1777 (2006).
- [10] E. E. Narimanov and A. V. Kildishev, *Appl. Phys. Lett.* **95**, 041106 (2009).
- [11] S. M. Vukovic, I. V. Shadrivov, and Y. S. Kivshar, *Appl. Phys. Lett.* **95**, 041902 (2009).
- [12] D. Ö. Güney and D. A. Meyer, *Phys. Rev. A* **79**, 1 (2009).
- [13] N. Papasimakis, V. Fedotov, and N. Zheludev, *Phys. Rev. Lett.* **101**, 253903 (2008).
- [14] C. Helgert, C. Menzel, C. Rockstuhl, E. Pshenay-Severin, E. B. Kley, A. Chipouline, A. Tünnermann, F. Lederer, and T. Pertsch, *Opt. Lett.* **34**, 704 (2009).
- [15] C. García-Meca, R. Ortuño, F. J. Rodríguez-Fortuño, J. Martí, and A. Martínez, *Opt. Lett.* **34**, 1603 (2009).
- [16] M. Thiel, G. von Freymann, S. Linden, and M. Wegener, *Opt. Lett.* **34**, 19 (2009).
- [17] B. Bai, Y. Svirko, J. Turunen, and T. Vallius, *Phys. Rev. A* **76**, 023811 (2007).
- [18] L. Arnaut, *J. Electromagn. Waves Appl.* **11**, 1459 (1997).
- [19] J. A. Reyes and A. Lakhtakia, *Opt. Comm.* **266**, 565 (2006).
- [20] S. Prosvirnin and N. Zheludev, *J. Opt. A: Pure Appl. Opt.* **11**, 074002 (2009).
- [21] S. Tretyakov, I. Nefedov, A. Shivola, S. Maslovski, and C. Simovski, *J. Electromagn. Waves Appl.* **17**, 695 (2003).
- [22] V. Fedotov, A. Schwanecke, and N. Zheludev, *Nano Lett* **7**, 1997 (2007).
- [23] S. V. Zhukovsky, S. V. Zhukovsky, A. V. Novitsky, A. V. Novitsky, V. M. Galynsky, and V. M. Galynsky, *Opt. Lett.* **34**, 1988 (2009).
- [24] V. Fedotov, P. Mladyonov, S. Prosvirnin, A. V. Rogacheva, Y. Chen, and N. I. Zheludev, *Phys. Rev. Lett.* **97**, 167401 (2006).
- [25] J. Pendry, *Science* **306**, 1353 (2004).

- [26] S. Tretyakov, A. Sihvola, and L. Jylhä, *Photonics Nanostruct. Fundam. Appl.* **3**, 107 (2005).
- [27] J. Zhou, J. Dong, B. Wang, T. Koschny, M. Kafesaki, and C. M. Soukoulis, *Phys. Rev. B* **79**, 1 (2009).
- [28] G. P. Ortiz, B. E. Martínez-Zérega, B. S. Mendoza, and W. L. Mochán, *Phys. Rev. B* **79** (2009).
- [29] L. Onsager, *Phys. Rev.* **37**, 405 (1931).
- [30] H. Casimir, *Rev. Mod. Phys.* **17**, 343 (1945).
- [31] S. Tretyakov, A. Sihvola, and B. Jancewicz, *J. Electromagn. Waves Appl.* **16**, 573 (2002).
- [32] S. Tretyakov, *Analytical Modeling in Applied Electromagnetics* (Artech House, Boston, 2003).
- [33] J. Petschulat, C. Menzel, A. Chipouline, C. Rockstuhl, A. Tünnermann, F. Lederer, and T. Pertsch, *Phys. Rev. A* **78**, 043811 (2008).
- [34] R. E. Raab and O. L. D. Lange, *Multipole Theory in Electromagnetism* (Clarendon, Oxford, 2005).
- [35] C. Rockstuhl, T. Zentgraf, E. Pshenay-Severin, J. Petschulat, A. Chipouline, J. Kuhl, T. Pertsch, H. Giessen, and F. Lederer, *Optics Express* **15**, 8871 (2007).
- [36] L. Lie, *J. Opt. Soc. Am. A* **14**, 2758 (1997).
- [37] B. Canfield, S. Kujala, M. Kauranen, K. Jemovs, T. Vallius, and J. Turunen, *Appl. Phys. Lett.* **86**, 183109 (2005).
- [38] B. Canfield, S. Kujala, K. Jefimovs, and T. Vallius, *J. Opt. A: Pure Appl. Opt.* **7**, 110 (2005).
- [39] G. Borzdov, *J. Math. Phys.* **38**, 6328 (1997).
- [40] H. Chen, L. Ran, J. Huangfu, X. Zhang, K. Chen, T. M. Grzegorzcyk, and J. A. Kong, *Appl. Phys. Lett.* **86**, 151909 (2005).
- [41] H. S. Chen, L. X. Ran, J. T. Huangfu, X. M. Zhang, and K. S. Chen, *Prog. Electromagn. Res.* **51**, 231 (2005).
- [42] E. Prodan, C. Radloff, N. Halas, and P. Nordlander, *Science* **302** (2003).
- [43] J. Petschulat, C. Menzel, A. Chipouline, C. Rockstuhl, A. Tünnermann, F. Lederer, and T. Pertsch, submitted to *Phys. Rev. Lett.* *Multipole Nonlinearity of Metamaterials*, 1 (2009).
- [44] P. B. Johnson and R. W. Christy, *Phys. Rev. B* **6**, 4370 (1972).
- [45] The period in x and y direction is $0.4 \mu\text{m}$, the SRR arm length $0.2 \mu\text{m}$, the base width $0.08 \mu\text{m}$, the arm width $0.04 \mu\text{m}$ and the metal film thickness $0.025 \mu\text{m}$. Au material data has been used according to [44]. As a substrate index we used $n_{\text{sub}} = 1.5$ and for the ambient

material $n_{\text{amb}} = 1$.

- [46] We mention that the fitting procedure can be performed manually since the parameters are distinct with respect to their spectral effect, e.g. resonance frequency (ω_0), resonance splitting (σ), resonance width (γ) and resonance strength ($q^2\eta\epsilon_0^{-1}m^{-1}$).